An Ad-Hoc Adaptive Pilot Model for Pitch Axis Gross Acquisition Tasks

Curtis E. Hanson
Dryden Flight Research Center, Edwards, California

NASA STI Program ... in Profile

Since its founding, NASA has been dedicated to the advancement of aeronautics and space science. The NASA scientific and technical information (STI) program plays a key part in helping NASA maintain this important role.

The NASA STI program operates under the auspices of the Agency Chief Information Officer. It collects, organizes, provides for archiving, and disseminates NASA's STI. The NASA STI program provides access to the NASA Aeronautics and Space Database and its public interface, the NASA Technical Reports Server, thus providing one of the largest collections of aeronautical and space science STI in the world. Results are published in both non-NASA channels and by NASA in the NASA STI Report Series, which includes the following report types:

- TECHNICAL PUBLICATION. Reports of completed research or a major significant phase of research that present the results of NASA Programs and include extensive data or theoretical analysis. Includes compilations of significant scientific and technical data and information deemed to be of continuing reference value. NASA counter-part of peer-reviewed formal professional papers but has less stringent limitations on manuscript length and extent of graphic presentations.

- TECHNICAL MEMORANDUM. Scientific and technical findings that are preliminary or of specialized interest, e.g., quick release reports, working papers, and bibliographies that contain minimal annotation. Does not contain extensive analysis.

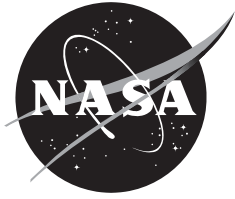- CONTRACTOR REPORT. Scientific and technical findings by NASA-sponsored contractors and grantees.

- CONFERENCE PUBLICATION. Collected papers from scientific and technical conferences, symposia, seminars, or other meetings sponsored or co-sponsored by NASA.

- SPECIAL PUBLICATION. Scientific, technical, or historical information from NASA programs, projects, and missions, often concerned with subjects having substantial public interest.

- TECHNICAL TRANSLATION. English-language translations of foreign scientific and technical material pertinent to NASA's mission.

Specialized services also include organizing and publishing research results, distributing specialized research announcements and feeds, providing information desk and personal search support, and enabling data exchange services.

For more information about the NASA STI program, see the following:

- Access the NASA STI program home page at http://www.sti.nasa.gov

- E-mail your question to help@sti.nasa.gov

- Fax your question to the NASA STI Information Desk at 443-757-5803

- Phone the NASA STI Information Desk at 443-757-5802

- Write to:
  STI Information Desk
  NASA Center for AeroSpace Information
  7115 Standard Drive
  Hanover, MD 21076-1320

NASA/TM—2012–216031

An Ad-Hoc Adaptive Pilot Model for Pitch Axis Gross Acquisition Tasks

Curtis E. Hanson
Dryden Flight Research Center, Edwards, California

September 2012

Abstract

An ad-hoc algorithm is presented for real-time adaptation of the well-known crossover pilot model and applied to pitch axis gross acquisition tasks in a generic fighter aircraft. Off-line tuning of the crossover model to human pilot data gathered in a fixed-based high fidelity simulation is first accomplished for a series of changes in aircraft dynamics to provide expected values for model parameters. It is shown that in most cases, for this application, the traditional crossover model can be reduced to a gain and a time delay. The ad-hoc adaptive pilot gain algorithm is shown to have desirable convergence properties for most types of changes in aircraft dynamics.

Nomenclature

dt	time step, seconds
$e^{-\tau s}$	time delay, seconds
G_c	controlled element (aircraft) transfer function, degrees per inch
G_c'	altered controlled element (aircraft) transfer function, degrees per inch
G_p	pilot model transfer function, inches per degree
HUD	heads-up display
k_q	pitch gain, degrees per second per inch
J	measure of fitness, inches^{-1}
K	pilot gain, inches per degree
ΔK	adaptive increment to the pilot gain, inches per degree
$\Delta \dot{K}^{(-)}$	decremental adaptive pilot gain rate of change, inches per degree per second
$\Delta \dot{K}^{(+)}$	incremental adaptive pilot gain rate of change, inches per degree per second
L_α	apparent lift-curve slope, seconds^{-1}
L^{-1}	multiplicative pitch gain uncertainty, unitless
NDI	non-linear dynamic inversion
PIO	pilot-in-the-loop oscillation
q	pitch rate, degrees per second
$\tilde{q}$	pitch rate tracking error, degrees per second
s	Laplace operator, seconds^{-1}
T_1	pilot lead time constant, seconds T_2 pilot lag time constant, seconds
α	lead-lag filter time constant scaling term, unitless
Γ_K	pilot gain adaptation rate, inches per degree per second
δ	pilot pitch stick deflection, inches
ε_θ	threshold scale factor on pitch angle error, unitless
ε_q	threshold scale factor on pitch rate, seconds
ζ_{sp}	short-period damping ratio, unitless
ζ_{sp}'	altered short-period damping ratio, unitless
θ	sensed pitch angle, degrees
θ_{cmd}	pitch angle command, degrees
$\tilde{\theta}$	pitch angle tracking error, degrees
μ_1	addative short period dynamics uncertainty, seconds^{-2}
μ_2	addative short period dynamics uncertainty, seconds^{-1}
τ	pilot's effective time delay, seconds
τ_θ	aircraft pitch response time delay, seconds
ω_{sp}	short-period natural frequency, seconds^{-1}
ω_{sp}'	altered short-period natural frequency, seconds^{-1}

Introduction

Mathematical models of piloting technique are valuable tools for aircraft designers and, in the case of modern fly-by-wire aircraft, for flight control designers as well. The latter case in particular has prompted efforts to model the pilot's behavioral response as a control system rather than the perhaps more realistic, but less analytically tractable approach of modeling the physical characteristics of the pilot as a biological system. Controls-oriented pilot models can be used to broadly categorize pilot dynamic behavior in terms of high-gain or low-gain response; provide a basis for understanding pilot techniques such as lead- or lag-compensation; and serve as a tool for studying the interactions between the pilot, the aircraft, and the flight control system. Methods for modeling pilot behavior as control systems can be found in reference 1 and 2.

Recent applications of adaptive flight control systems to aircraft (refs. 3 and 4) have demonstrated their potential for adverse pilot-controller interactions, such as pilot-in-the-loop oscillations (PIOs). Historically these types of events, also called aircraft-pilot coupling, have been an infrequent, yet potentially serious risk associated with flight test and operation of piloted aircraft. Adaptive controllers are primarily concerned with variations in plant dynamics, whether due to changes in the vehicle such as those caused by failures or damage, or its environment as in the case of changing flight conditions. When changes to plant dynamics are objectionable, the pilot may also become an adaptive element. Therefore, a thorough analysis of interactions between the pilot and the adaptive controller requires an adaptive model of the pilot that is reasonably representative.
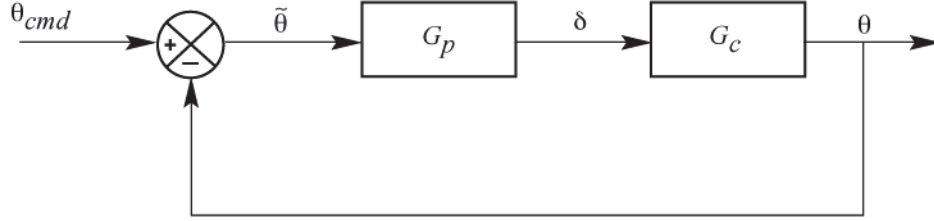
There is very little published work on adaptive pilot models. One recent effort (ref. 5) has applied an ad-hoc adaptation algorithm to a pilot pursuit model. This model contains a fixed transfer function of the pilot's neuromuscular system and two adaptive gains, one corresponding to rate feedback and the other to position feedback. The ad-hoc update law adjusts the rate feedback gain based upon error between the commanded rate and the rate feedback. The position feedback gain is adjusted proportionally to changes in the rate gain. This algorithm was shown to have good adaptation characteristics for a variety of example problems, primarily consisting of switching between the dynamics of different simple systems. However, it relies upon explicit knowledge of the time at which a change in plant dynamics occurs and only allows for a brief period of adaptation. The variable gains are prone to large instantaneous changes caused by the use of a threshold function that is not representative of a human pilot. Furthermore, the position feedback gain adjustment is only allowed to increase, preventing adaptation to situations in which the change in plant dynamics is only temporary.

This report presents an ad-hoc method for adapting the well-known crossover pilot model applied to the pitch axis control of a generic fighter aircraft. This new method improves upon the technique of (ref. 5) by allowing continuous, smooth adaptation for both gain increases and decreases to provide a better match for human pilot behavior. First, a description of the pilot-vehicle system is presented for a pitch angle gross-acquisition task. A suite of altered aircraft dynamics is then introduced to analyze changes in pilot technique due to changes in plant behavior. The fixed-gain crossover pilot model is fit to human pilot data from a ground-based high-fidelity simulation for each of these cases, and the resulting model parameters and associated frequency and time responses are analyzed. It is shown that in most cases a simplified form of the pilot model provides a sufficient match to the human pilot data. An adaptive algorithm for adjusting the gain of the simplified pilot model is synthesized from the results of this analysis, and simulation data of real-time pilot model adaptation is presented.

Pilot-Vehicle System Description

The block diagram shown in figure 1 represents the pilot-vehicle system for a pitch axis gross acquisition task. In this case, a series of pitch angle commands θ_{cmd} are provided to the pilot, presumably

through a visual display. In a similar fashion, the aircraft pitch angle θ is observed by the pilot who forms a mental estimate of the pitch angle error $\tilde{\theta}$. Compensation is then applied via the pilot model G_p in the form of a control stick deflection, which in turn drives the aircraft pitch angle according to the vehicle dynamics G_c.

Figure 1. Pilot-vehicle system for a short-period gross acquisition task.

The pilot model G_p is the primary subject of this report and is discussed in detail in the sections that follow. The vehicle dynamics G_c, described by equation (1), are the pitch-axis short-period dynamics for a typical modern fighter aircraft (ref. 6).

$$G_c = \frac{\theta}{\delta} = k_q \frac{\omega_{sp}^2(s + L_\alpha)}{(s^2 + 2\zeta_{sp}\omega_{sp}s + \omega_{sp}^2)s} \tag{1}$$

The results presented in this report were obtained using a high-fidelity F-18 aircraft (McDonnell Douglas now The Boeing Company, Chicago, Illinois) simulation in which equation (1) formed the reference model for a non-linear dynamic inversion (NDI) control law. The NDI controller suppressed the natural dynamics of the F-18 aircraft and replaced them with the desired reference dynamics. Nominal values for the constant terms of equation (1) were selected to provide Level 1 flying characteristics. Reference 7 defines Level 1, or satisfactory, flying qualities as, "Flying qualities adequate for the mission Flight Phase. Desired performance is achievable with no more than minimal compensation."

An investigation of pilot adaptation and the corresponding development of an adaptive pilot model requires the ability to vary the aircraft dynamics in a predictable and precise manner. The nominal reference model dynamics were augmented according to equation (2) with three uncertainty terms L^{-1}, μ_1, and μ_2 which could be altered in combinations to produce variations in loop gain, frequency, and damping as desired. The alternate dynamics scenarios which were investigated are listed in table 1.

$$G_c' = \frac{\theta}{\delta} = L^{-1}k_q \frac{\omega_{sp}^2(s + L_\alpha)}{\left(s^2 + \left(2\zeta_{sp}\omega_{sp} + \mu_2\right)s + \left(\omega_{sp}^2 + \mu_1\right)\right)s} \tag{2}$$

Table 1. Scenarios for changes in vehicle dynamics.

Scenario	L^{-1}	μ_1	μ_2	Description
I	1	0	0	nominal aircraft dynamics
II	0.5	0	0	50% reduction in loop gain
III	2.0	0	0	100% increase in loop gain
IV	1	0	-1.8428	reduction in damping ratio, $\zeta'_{sp} = 0.2$
V	1	0	4.146	increase in damping ratio, $\zeta'_{sp} = 1.0$
VI	0.2855	-10	-1.555	reduction in frequency, $\omega'_{sp} = 2.0$
VII	2	14.01	1.3836	increase in frequency, $\omega'_{sp} = 5.3$

Handling qualities predictions for each scenario in table 1 are shown in figure 2, based on the Neal-Smith criterion (ref. 8). Neal-Smith uses a pilot compensation transfer function consisting of lead-lag compensation and pilot gain to track pitch angle commands. These elements are adjusted to achieve a combination of desirable steady-state closed-loop error characteristics (3 dB droop) and specified bandwidth frequency. A range of bandwidth frequencies, between 1.5 and 3.5 radians per second were analyzed with an assumed pilot lag of 300 milliseconds. The magnitude of the required phase compensation and closed-loop resonant peak are cross-plotted against Level 1, 2, and 3 boundaries that have been derived from historical flight data.
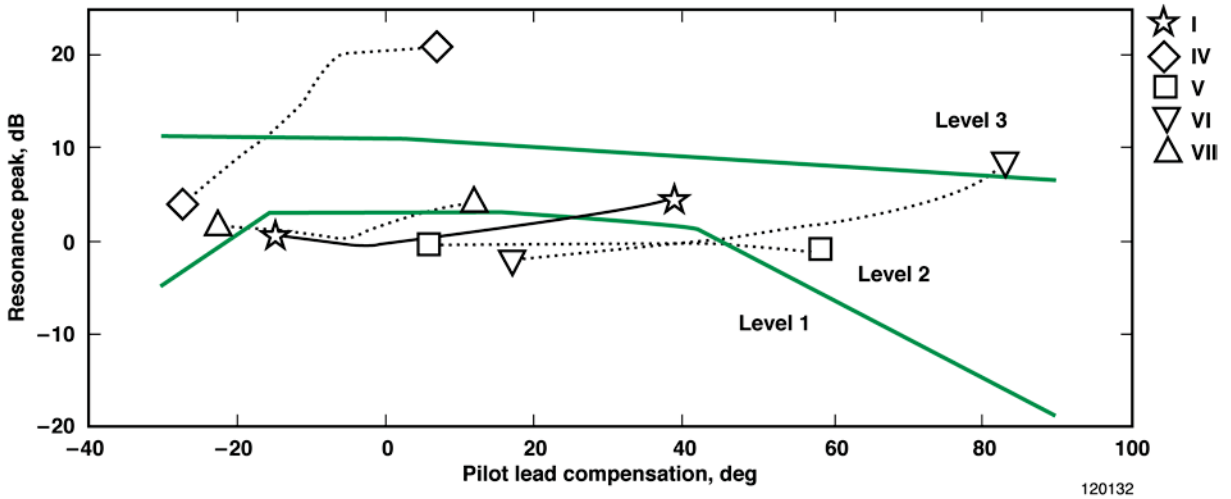

Figure 2. Handling qualities predictions for alternate dynamics scenarios using the Neal-Smith criteria.

The baseline aircraft dynamics, as well as the increased damping ratio and reduced natural frequency cases (scenarios I, V, and VII respectively) all show mostly Level 1 predictions with little sensitivity of the resonance peak to variations in pilot bandwidth. The Neal-Smith predictions for changes to the loop gain (scenarios II and III) did not vary significantly from the predictions for the baseline case and are not shown.

The Neal-Smith criterion predicts the reduced pitch damping dynamics (scenario IV) to be solidly Level 2 for low bandwidth tasks. Increasing the bandwidth raises the magnitude of the resonance peak and pushes the predictions into the upper-left corner of the criterion's Level 3 region, which indicates a strong potential for PIO tendencies due to abrupt aircraft responses.

4

A decrease in the natural frequency response of the aircraft (scenario VI) results in Level 1 handling qualities predictions for low bandwidth tasks and Level 3 for high bandwidth tasks. As with scenario IV, Neal-Smith predicts scenario VI to be PIO prone, but in this case caused by a combination of resonant peak and an excessively sluggish response.

Fixed-Gain Crossover Pilot Model Description

The basis for the adaptive pilot model developed in this paper is a modification of the pilot crossover model, the traditional form of which (ref. 1) is described in equation (3). The traditional model consists of a pilot gain K, lead time constant T_1, lag time constant T_2, and effective time delay τ. The adaptive model eliminates the lead and lag time constants in order to simplify the adaptation algorithm, a modification that is justified below through comparisons with human pilot data.

$$G_p = \frac{\delta}{\tilde{\theta}} = K \frac{T_1 s + 1}{T_2 s + 1} e^{-\tau s} \tag{3}$$

The crossover model can be re-arranged, as in equation (4), to yield an expression for the pilot's pitch stick command as a function of the pitch angle and pitch rate tracking errors. The pilot lag time constant T_2 has been re-written in terms of the lead time constant T_1 and a non-negative scalar term α. A value of $\alpha < 1$ denotes pilot lead compensation while $\alpha > 1$ indicates pilot lag compensation.

$$\delta = K\left(T_1 \tilde{q} + \tilde{\theta}\right) \left(\frac{1}{\alpha T_1 s + 1}\right) e^{-\tau s} \tag{4}$$

Note that, setting either $\alpha = 1$ or $T_1 = 0$ in equation (4) has the effect of eliminating the lead-lag filter from the pilot model, leaving only the gain and time delay. Also, to avoid unrealistically small filter time constants α was set to zero in the event that the combined term $\alpha T_1 < 0.025$. The value of 0.025 was chosen as four times the simulation fixed step size to provide adequate margin from the Nyquist frequency.

The pilot's effective time delay represents the unavoidable delay between sensing an error and manipulating the control stick, combining elements such as reaction time and neuromuscular lag. Because this feature of the crossover model is an unalterable characteristic of the pilot, it was not made an adaptable parameter. Typical values for the effective time delay between 300 and 400 milliseconds were determined from the piloted simulation by measuring the delay between the initial movement of a tracking target to the initial deflection of the pitch stick. The effective time delay was implemented as a first-order Padé approximation.

For each of the scenarios described in table 1, the parameters of the crossover pilot model were tuned via a non-linear search routine to match as closely as possible the piloting technique of a single human subject in NASA Dryden's piloted F-18 aircraft simulation. A gross acquisition task was used as shown in figure 3, consisting of a series of pitch angle captures. Using the heads-up display (HUD), the pilot attempted to place a circular body-axis-fixed pipper onto a vertically-displaced target line. Tracking error is the difference in elevation angle between pipper and target line. The resulting crossover model parameter sets are listed in table 2. In all seven cases it can be seen that $\alpha > 1$, indicating various degrees of pilot lag compensation. In some cases the lag compensation is at very high frequency and doesn't affect the tracking performance.

Table 2. Crossover model parameter fits to human subject data.

Scenario	K	T_1	α	Description
I	0.16	0.0013	43	nominal aircraft dynamics
II	0.34	0.101	2	50% reduction in loop gain
III	0.082	0.0042	9	100% increase in loop gain
IV	0.20	0.33	2.7	reduction in damping ratio
V	0.22	0.017	1.5	increase in damping ratio
VI	0.50	0.35	1.4	decrease in frequency
VII	0.80	0.58	2.1	increase in frequency

Figure 3. HUD pitch angle gross acquisition task.

The applicability of the pilot crossover model parameter sets in table 2 for each scenario was evaluated according to the similarity between the pilot model's pitch stick commands δ^{model} and the human subject pilot's commands δ^{pilot} for a given task. Figure 4 shows the best and worst matches as calculated from the fitness function described in equation (5).

$$J = \frac{1}{1 + \left\| \sqrt{\int (\delta^{pilot} - \delta^{model})^2} \right\|_\infty} \tag{5}$$
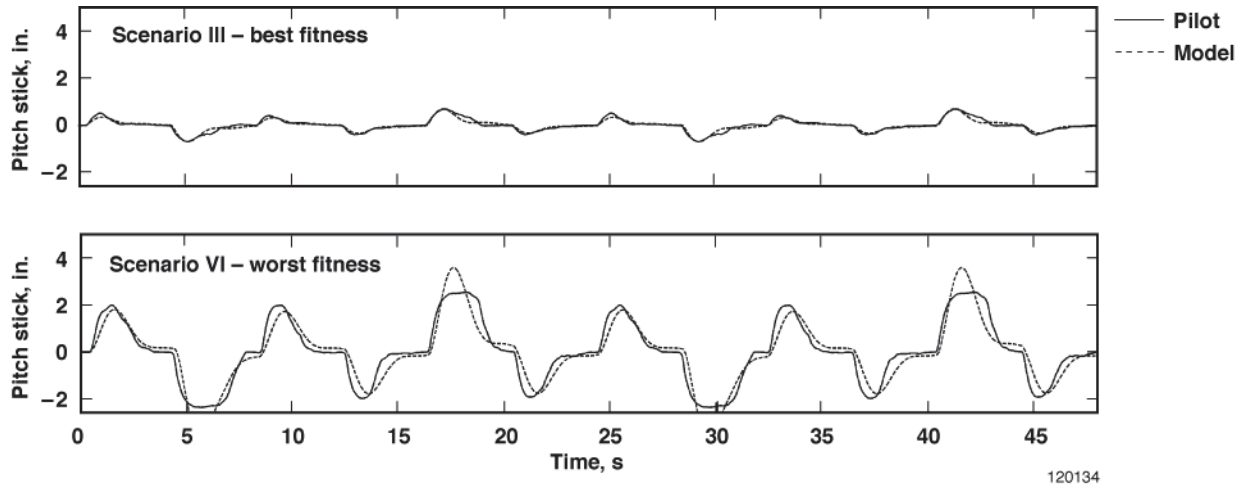

Figure 4. Sample matches between human pilot and crossover model commands.

6

Even for scenario VI, which had the worst match, the tuned crossover model closely matches the human subject's piloting technique with some lag and tendency to overshoot. It should be noted that human pilots display a wide range of piloting techniques, and even the same pilot may fly differently in different situations. The parameter sets in table 2 are not intended to apply to all pilots in all situations. However, the intent of this report is to show that the traditional crossover pilot model can be tuned to match a given set of human subject data. Later, it will be shown that the pilot model can be made self-tuning. In both cases, the results are specific to the human subject pilot for which the data was collected. Data for another pilot with a different piloting technique would likely produce different parameter sets and different adaptation characteristics. The extent to which the algorithms presented here apply to a general population of human pilots remains a topic for further research.

Analysis of Scenario I – Nominal Aircraft Dynamics

The crossover model derives its name from a rule-of-thumb (ref. 1), which states that a pilot will typically apply manual compensation such that the frequency response magnitude of the open-loop pilot-vehicle system $|G_p G_c|$ exhibits a slope of approximately -20 dB per decade in the region of the 0 dB crossover. This rule-of-thumb is illustrated in figure 5. The magnitude response curves are shown for the nominal short-period aircraft dynamics without pilot compensation (G_c) and for the combined pilot-vehicle system ($G_p G_c$). The crossover pilot model parameters used in this case correspond to scenario I in table 2. It is clear from figure 5 that the un-compensated open-loop short-period dynamics have a crossover slope of -40 dB per decade, and that the effect of pilot compensation is to lower the loop gain by approximately 16 dB, reducing the open-loop crossover frequency to a region at which the magnitude slope is nearly -20 dB per decade.
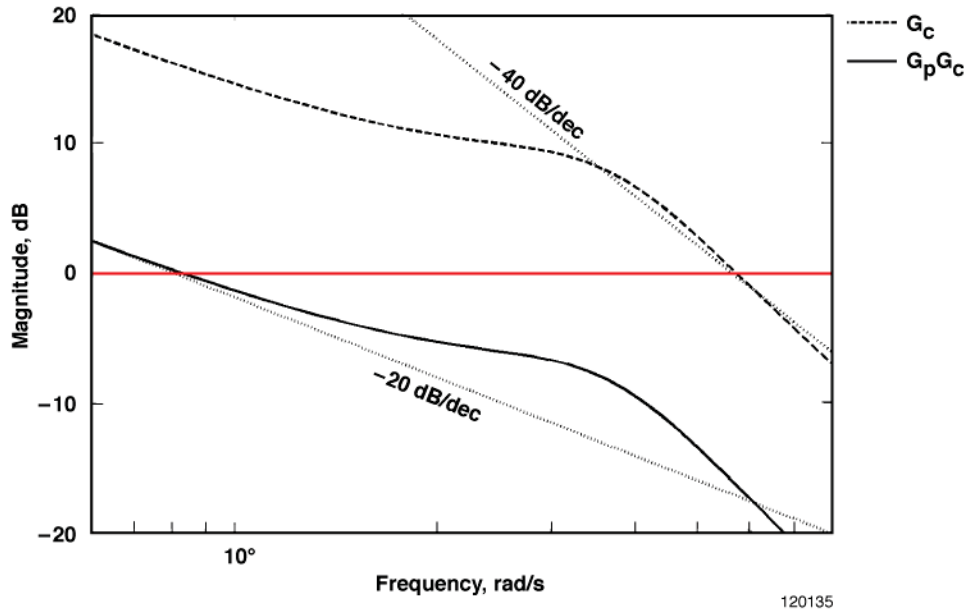

Figure 5. Change in open-loop crossover slope due to pilot compensation.

From table 2 it is apparent that the human subject pilot applied a very small amount of lag compensation in addition to lowering the loop gain. Figure 6 shows through a series of five degree pitch angle captures that setting T_1 to zero in the pilot model results in no appreciable difference in command or response, indicating that for nominal airplane dynamics the pilot can be modeled as a gain and a time delay.
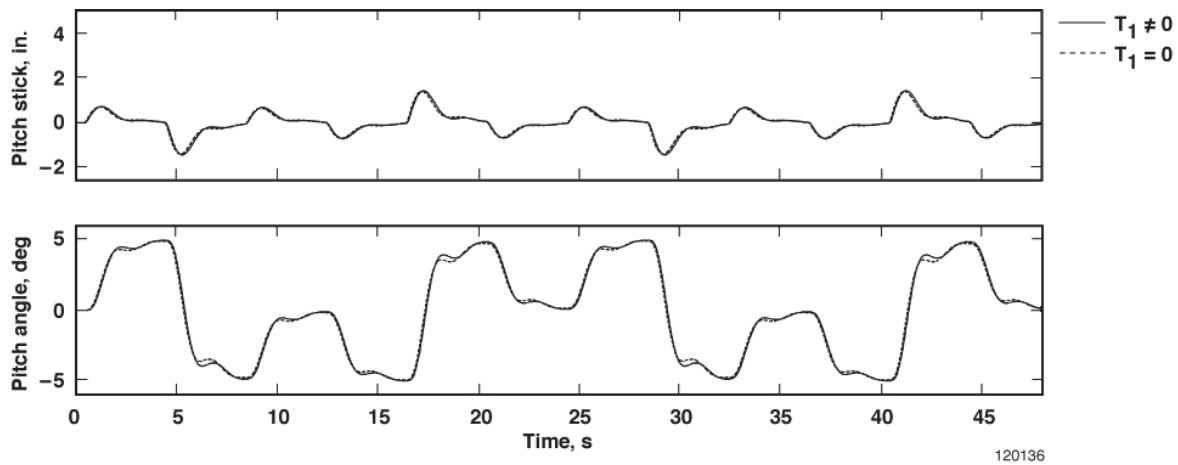
Figure 6. Effect of pilot model lag-lead in scenario I.

Analysis of Scenarios II and III – Changes in Loop Gain

Scenarios II and III both involve changes to the loop gain $L^{-1}k_q$ in equation (2). In these cases the compensating technique is to increase or decrease the pilot's gain K accordingly. From the values listed in table 2, the pilot gain for scenario II is doubled in value in comparison to scenario I to counter the 50 percent reduction in loop gain. Similarly, the 100 percent increase in loop gain for scenario III results in a reduction of the pilot gain by approximately half. Figure 7 shows that the pilot-compensated open-loop frequency response magnitudes for scenarios I, II, and III are nearly identical. The slight increase in high-frequency attenuation for scenario II is a result of the significantly larger value of T_1 and smaller value of α (refer again to table 2) in this case. However, as figure 8 shows, this increased lag-lead compensation is a minor contributor to the total pilot command. Therefore, as with scenario I, it is reasonable to model the pilot with a gain and a time delay for scenarios involving merely a change in the loop gain.
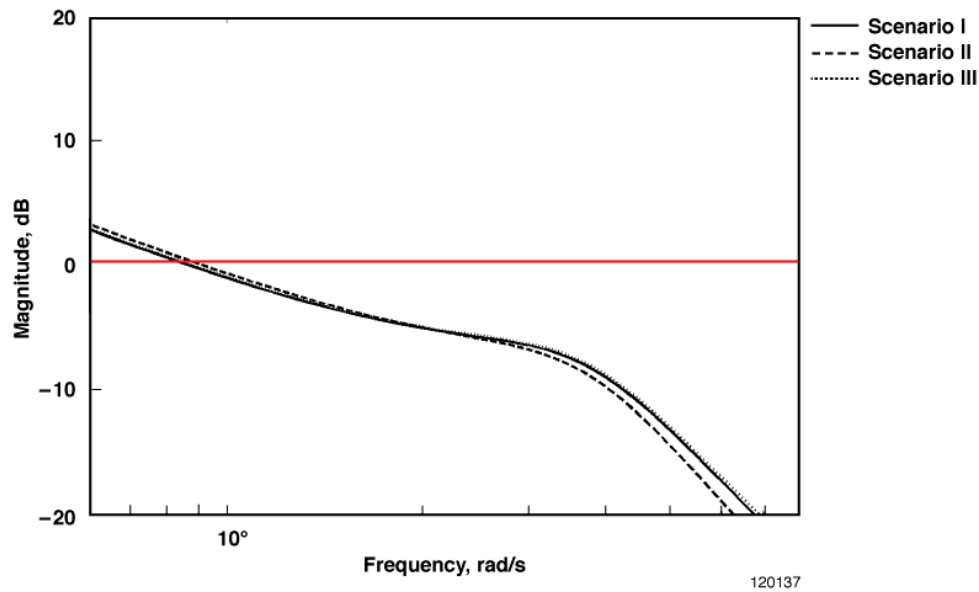

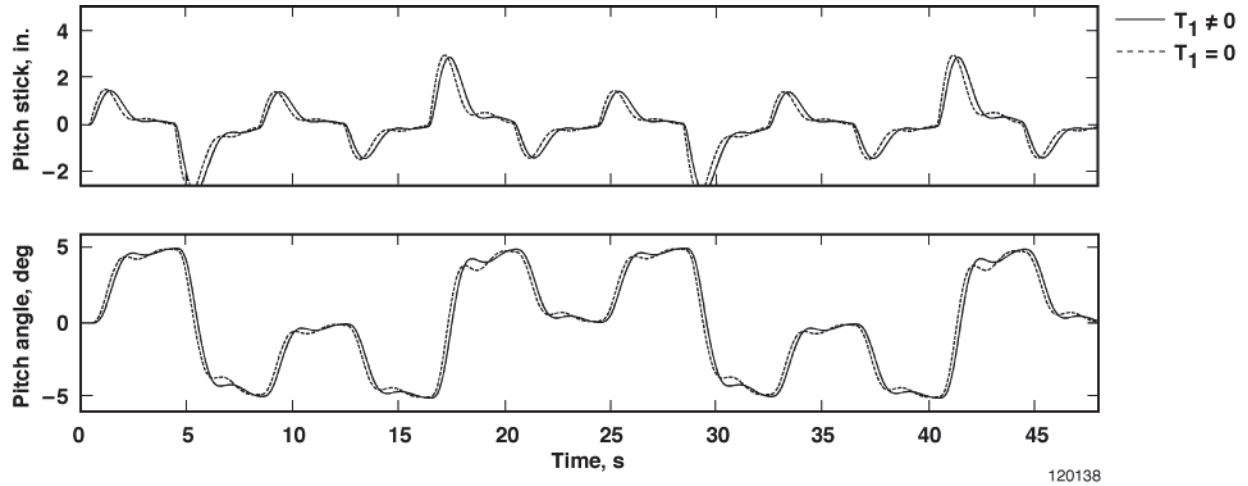Figure 7. Pilot-compensated frequency responses for changes in loop gain.

8

Figure 8. Effect of pilot model lag-lead in scenario II.

Analysis of Scenarios IV and V – Changes in Damping Ratio

The values in table 2 show that the human subject's piloting technique for the increased damping ratio of scenario V is similar to the technique employed for nominal airplane dynamics, with slightly less gain attenuation, that is a larger value of K. A small value for T_1 and a value for α close to unity, both indicate that lag-lead compensation is not used to any significant degree. As illustrated in figure 9, the increased damping of scenario V eliminates the resonant peak at the natural frequency ω_{sp} for the short period dynamics without pilot compensation. Consequently the dynamics do not exhibit the shallow (compared to -20dB per decade) slope at frequencies just below ω_{sp}, and the desired -20dB per decade slope is achieved with less pilot gain attenuation. For cases involving an increase in short period damping, the pilot can once again be modeled as a gain and a time delay.
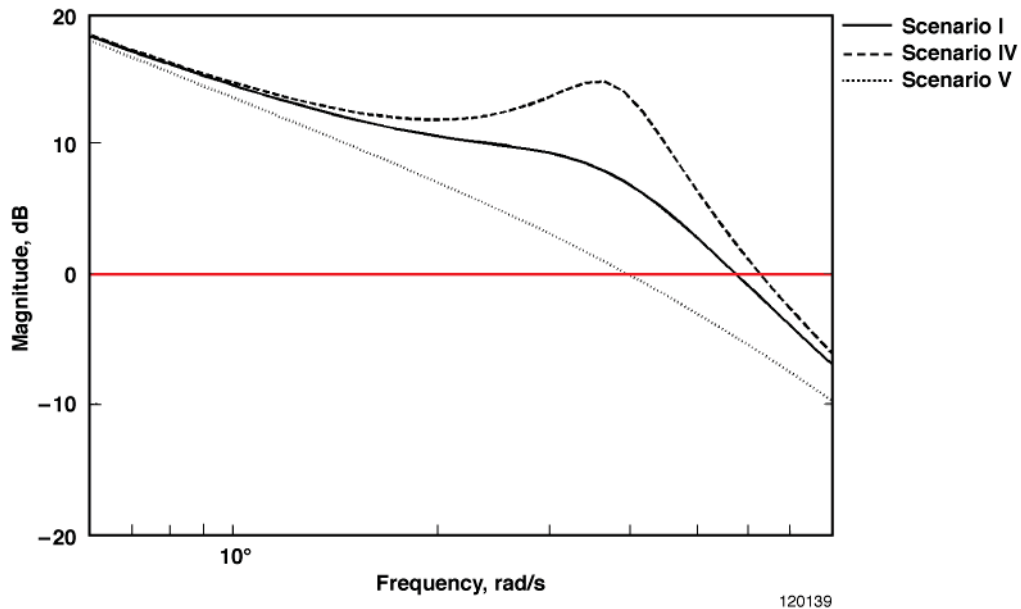

Figure 9. Short period (G_c) frequency response with variations in damping ratio.

9

A decrease in short period damping has the effect of amplifying the natural frequency resonant peak. From figure 10 it is apparent that the effect of the pilot's lag-lead compensation is to suppress the peak to approximately -6 dB while maintaining a crossover slope of -20 dB per decade. Eliminating the lag-lead compensator by setting T_1 to zero produces a crossover slope that is too shallow and raises the resonant peak back above the 0db line. It is interesting to note that reducing the pilot gain K for scenario IV in table 2 by 50 percent and leaving T_1 at zero produces the desired crossover slope and peak attenuation, but at the cost of reduced bandwidth.

Figure 11 shows the time-history response for the original scenario IV parameter values in table 2 compared with the responses obtained by eliminating the lag-lead compensation and by decreasing the pilot gain by 50 percent. The reduced bandwidth of the pilot model without lag-lead compensation clearly results in poorer performance during the pitch angle captures. However, this might be a reasonable piloting technique, especially in cases where the pilot's auxiliary workload is high or the pilot is distracted, and when a reduced bandwidth is acceptable to achieve the given task satisfactorily. Therefore, in some instances it may be acceptable to model the pilot as a gain and a time delay, even in cases of lightly damped pitch response.
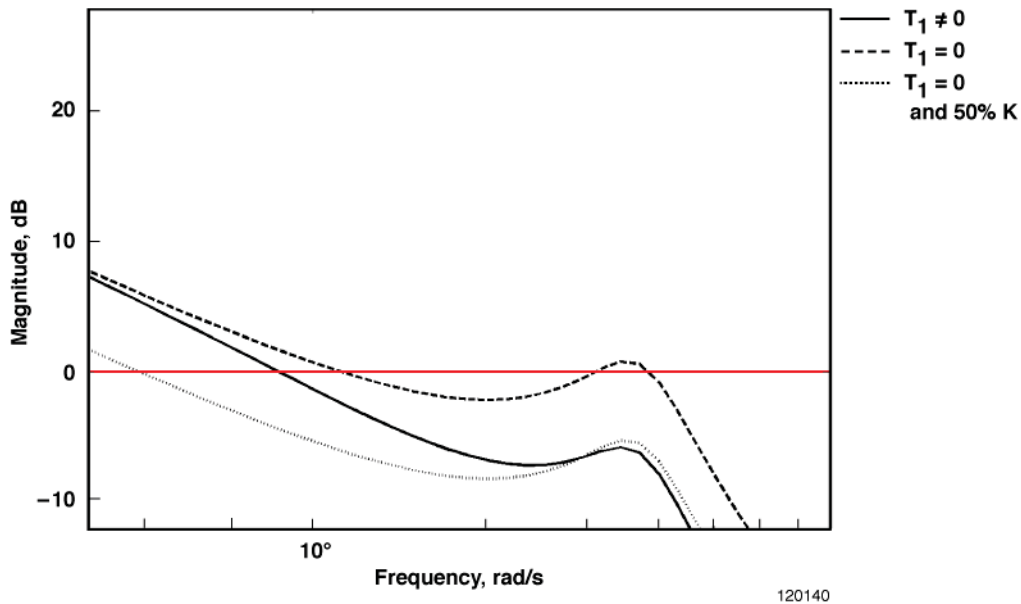

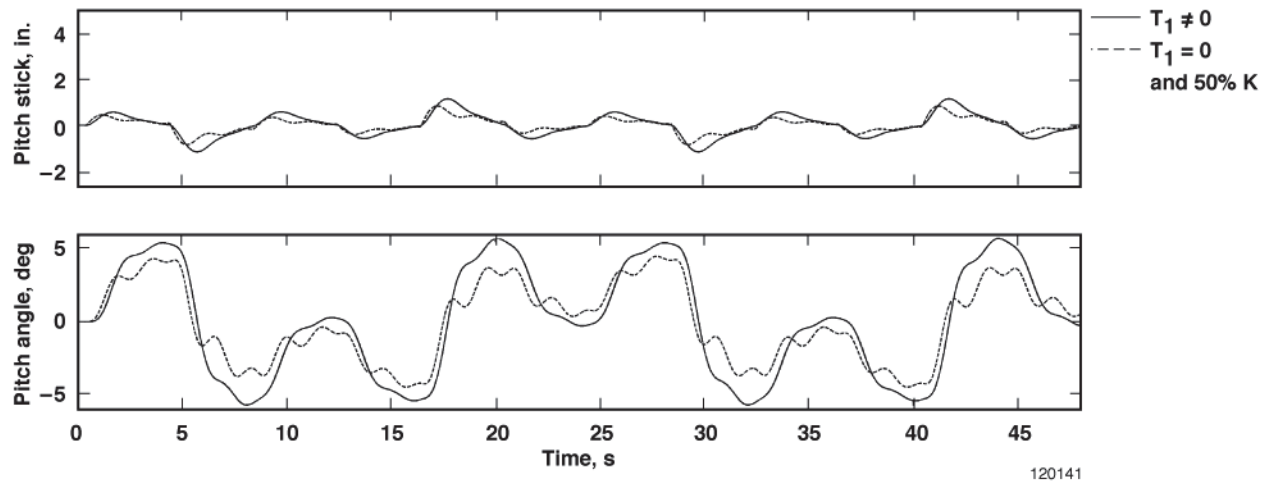Figure 10. Effect of lag-lead and gain changes on lightly-damped frequency response.

Figure 11. Effect of pilot lag-lead and gain compensation for scenario IV.

Analysis of Scenarios VI and VII – Changes in Natural Frequency

Altering the short period natural frequency primarily changes the aircraft's open-loop bandwidth, or crossover frequency. In order to achieve the same -20dB per decade slope it would seem reasonable that the pilot would apply a gain reduction as in the case of the nominal dynamics. The values for scenario VI in table 2 indicate that the human subject pilot applied far less gain attenuation than for the nominal case in scenario I. The corresponding frequency response, shown in figure 12, exhibits a crossover slope of nearly -40dB per decade and a crossover frequency much higher than for the nominal case. It is interesting to note that the two frequency responses in figure 12 cross each other near the original short period frequency ω_{sp} and at a magnitude of approximately minus 6dB. The applied pilot technique in this case appears to give greater weight to generating the desired attenuation at ω_{sp} than either crossover slope or crossover frequency.
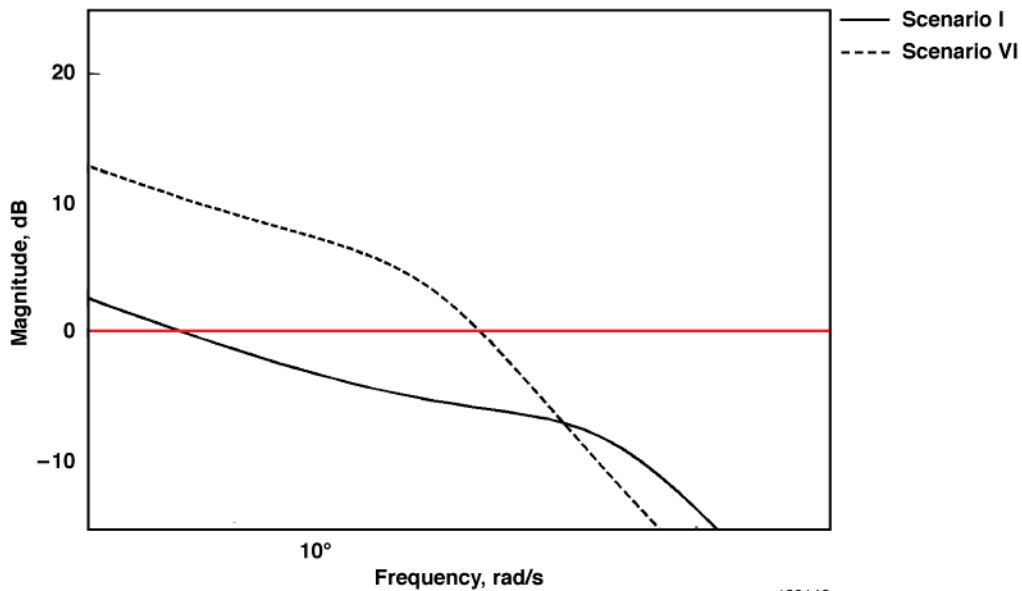

Figure 12. Pilot-vehicle frequency response for reduced frequency.

Although the value of T_1 in table 2 is relatively large for scenario VI, the corresponding value of α is only slightly larger than unity indicating that the pilot applied some damping to the closed-loop dynamics. As shown in figure 13, the time history response without the lead-lag filter active is slightly more oscillatory than with it. However, the degree of similarity between the time histories in figure 13 implies that pilot technique for cases of reduced natural frequency may be sufficiently approximated with just a pilot gain and effective delay.
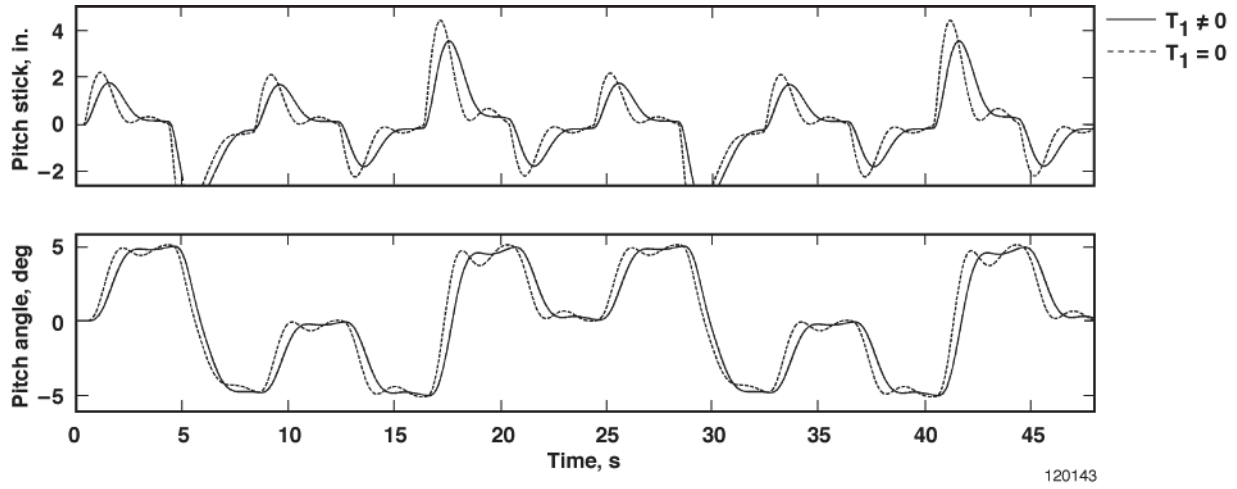
Figure 13. Effect of lag-lead compensation on scenario VI.

In the case of increased natural frequency, figure 14 shows that the human subject parameters for scenario VII in table 2 ($K = 0.8$) achieve a crossover slope of -20dB per decade, but only in the brief transitory range near the increased natural frequency ω'_{sp}. A further reduction of the pilot loop gain ($K = 0.3$) reduces the crossover frequency to a region in which the -20dB per decade slope is sustained over a wider frequency range.
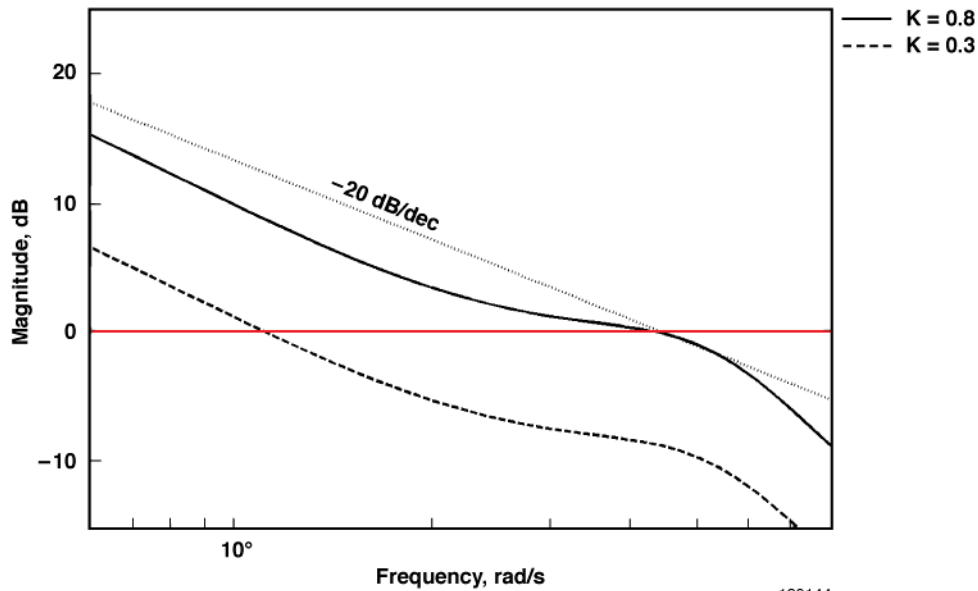
Figure 14. Pilot-vehicle frequency response for scenario VII.

12

For the pilot model parameters in table 2 corresponding to scenario VII, the lag-lead compensation is critical to the performance of the pilot-vehicle system; without it the natural frequency resonant peak is not sufficiently attenuated. When the pilot gain is reduced to $K = 0.3$, the lag-lead compensation can be removed while maintaining reasonable performance, as shown in figure 15. Therefore, in cases of either reduced or increased short period natural frequency, the pilot can be reasonably modeled as a gain and a time delay.
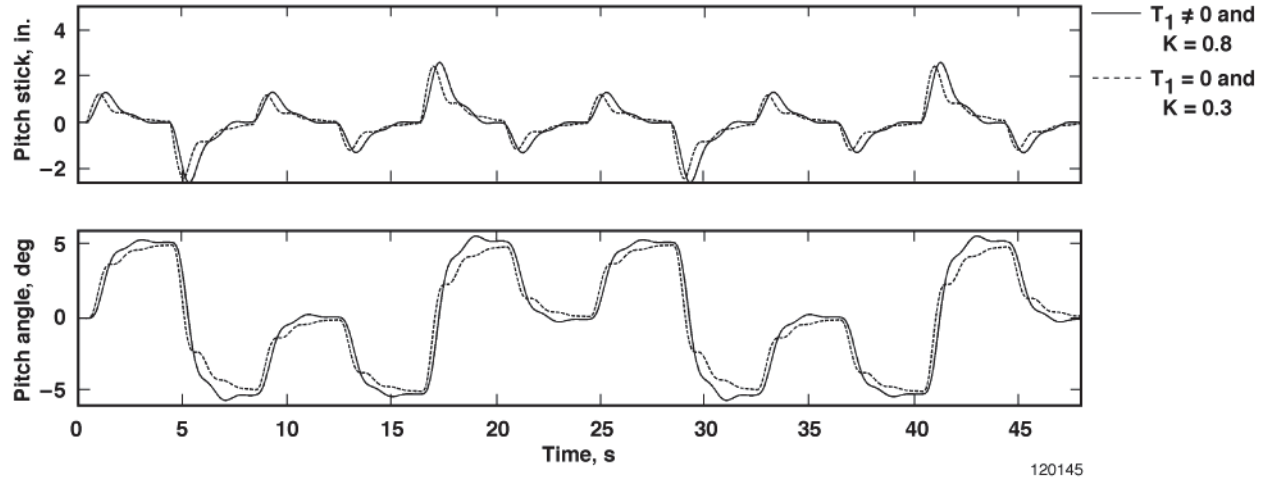

Figure 15. Effect of pilot model gain and lag-lead filter on scenario VII.

Adaptive Crossover Pilot Model Description

The crossover pilot model is made adaptive, or self-tuning, by adding an adjustable increment to the pilot gain. Attempts were made to add adaptive increments to T_1 and α as well, but a set of ad hoc adaptive rules for them could not be satisfactorily determined and remain a topic to be investigated. However, as the fixed-gain pilot model analysis demonstrated, the pilot can generally be considered as a gain and a time delay for the scenarios investigated in this report. Therefore, the adaptive crossover pilot model takes the form shown in equation (6).

$$\delta = (K + \Delta K)\tilde{\theta}e^{-\tau s} \tag{6}$$

The rules described in this section for computing the adaptive increment to the pilot gain were developed in an ad hoc manner. There is no formal derivation, nor are there formal stability proofs for them. However, they will be shown in certain cases to approximate the changes in piloting technique displayed by human pilots in response to modifications in system dynamics.

Adaptation Algorithm for the Pilot Gain

The incremental pilot gain is computed by integrating the sum of negative and positive rate of change terms, described by equation (7).

$$\Delta K = \int \left(\Delta \dot{K}^{(-)} + \Delta \dot{K}^{(+)} \right) dt \tag{7}$$

The individual terms for negative and positive rates of change of the pilot gain, $\Delta \dot{K}^{(-)}$ and $\Delta \dot{K}^{(+)}$ respectively, are calculated according to equation (8). The pilot gain adaptation is a function of the

difference between the pitch angle tracking error $\tilde{\theta}$ and the derivative of the associated feedback, $\dot{\theta} \cong q$. This error signal is similar to the one used by reference 5.

$$
\Delta \dot{K}^{(-)} = \begin{cases} 0, & |\tilde{\theta}|e^{-\tau_\theta s} \leq \varepsilon_\theta^{(-)}(1 + |\theta_{cmd}|e^{-\tau_\theta s}) \\ 0, & |\tilde{\theta}|e^{-\tau_\theta s} - \varepsilon_q^{(-)}|q| \geq 0 \\ \Gamma_K^{(-)} \dfrac{|\tilde{\theta}|e^{-\tau_\theta s} - \varepsilon_q^{(-)}|q|}{1 + |\theta_{cmd}|e^{-\tau_\theta s}}, & \text{otherwise} \end{cases}
\tag{8}
$$

$$
\Delta \dot{K}^{(+)} = \begin{cases} 0, & |\tilde{\theta}|e^{-\tau_\theta s} \leq \varepsilon_\theta^{(+)}(1 + |\theta_{cmd}|e^{-\tau_\theta s}) \\ 0, & |\tilde{\theta}|e^{-\tau_\theta s} - \varepsilon_q^{(+)}|q| \leq 0 \\ \Gamma_K^{(+)} \dfrac{|\tilde{\theta}|e^{-\tau_\theta s} - \varepsilon_q^{(+)}|q|}{1 + |\theta_{cmd}|e^{-\tau_\theta s}}, & \text{otherwise} \end{cases}
$$

The two similar sets of conditional statements applied to $\Delta \dot{K}^{(-)}$ and $\Delta \dot{K}^{(+)}$ in equation (8) can be understood as ensuring that pilot gain adaptation occurs when the following statements are true.

1. The pitch angle error is large in comparison to the command (indicating that a gain adjustment may be necessary to improve tracking), and
2. The pitch rate response is outside an acceptable range of aggressiveness, which linearly decreases with decreasing tracking error.
   a. Reduce the pilot gain if the slope of the pitch angle response is too steep, or
   b. Increase the pilot gain if the slope of the pitch angle response is too shallow.

The free design parameters of equation (8) are listed in table 3 along with their assigned values. These values were determined using a non-linear search routine and time history data of a human subject adapting to changes in loop gain. It was found that restricting the tuning search to the first three scenarios in table 1 significantly sped up the search process while producing parameter values that worked well for all seven scenarios. The tuning process attempted to minimize the norm of the differences between the human subject's pitch angle and pitch rate tracking as compared to those of the adaptive pilot model. The task was to perform a series of pitch angle captures with nominal aircraft dynamics (scenario I) followed by an identical series with uncertain dynamics (scenarios II and III). For the human subject data, this sequence was performed six times and the results were averaged together to ensure a typical response. During evaluation of the adaptive pilot model, the pilot gain was initialized to zero.

The time delay $e^{-\tau_\theta s}$ in equation (8) eliminates some of the difference between $\tilde{\theta}$ and q that arises due to system delays and phase loss, mimicking the ability of a human pilot to mentally perform phase-correlation between perceived error and resulting response. Alternatively, reference 5 used a root-mean-square (RMS) function to estimate the magnitude of expected error, and only permitted adaptation when the instantaneous error significantly exceeded the RMS error.

Table 3. Adaptive pilot model gain parameters.

Free Parameter	Tuned Value
τ_θ	0.34
$\varepsilon_\theta^{(-)}$	0.26
$\varepsilon_\theta^{(+)}$	0.29
$\varepsilon_q^{(-)}$	0.65
$\varepsilon_q^{(+)}$	1.53
$\Gamma_K^{(-)}$	3.4
$\Gamma_K^{(+)}$	1.1

Unique sets of threshold values $\varepsilon_\theta > 0$ and $\varepsilon_q > 0$ are applied when computing $\Delta\dot{K}^{(-)}$ and $\Delta\dot{K}^{(+)}$. The threshold ε_θ prevents adaptation when the pitch angle θ is within a threshold region near the pitch angle command, that is, when the pitch angle error $\tilde{\theta}$ is small, as illustrated in figure 16.
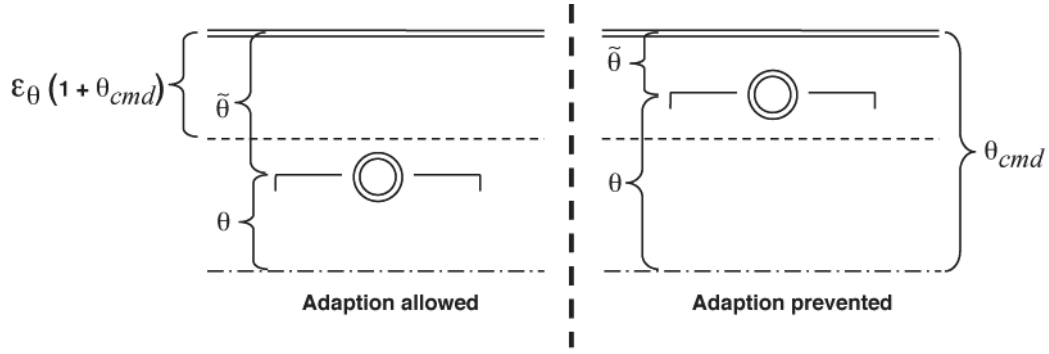

Figure 16. Illustration of pitch error threshold.

Large pitch angle error is a necessary, but not sufficient condition for adaptation. In other words, if the pitch angle error is large, but the aircraft is responding appropriately to the pilot model's corrective input, the pilot model gain should not change. The threshold ε_q regulates adaptation when the aircraft response is not appropriate for the degree of tracking error. Reductions in the pilot gain, $\Delta\dot{K}^{(-)} > 0$, are only permitted when the pitch rate response of the aircraft is excessively large in relation to the pitch angle error. This condition implies overly aggressive control and indicates that the pilot gain is too large. Conversely, if the pitch rate response of the aircraft is small relative to the magnitude of the error, the current level of pilot control input is insufficient to regulate the error and the pilot gain is permitted to increase, $\Delta\dot{K}^{(+)} > 0$.

The learning rates $\Gamma_K^{(-)}$ and $\Gamma_K^{(+)}$ control the rate of pilot gain adaptation. The error signal $\tilde{\theta}e^{-\tau_\theta s} - \varepsilon_q q$ is normalized with the magnitude of the pitch angle command to promote consistent adaptation characteristics for any size input.

Simulation Results for Pilot Gain Adaptation

The scenarios in table 1 were evaluated again in the 6DOF simulation with the same pitch attitude command sequence, except this time with the pilot gain K initialized to zero and the incremental pilot

gain ΔK computed real time according to the adaptive algorithm in equations (7) and (8). The lead time constant T_1 in all cases was set to zero to eliminate the lead-lag filter, yielding the adaptive pilot model in equation (6).

The simulation results for scenarios I, II, and III in figure 17 show several desirable characteristics of the adaptive algorithm. First, the adaptive gain reaches a quasi-steady state value with only minor fluctuations following the initial large change in value. Second, the steady-state values achieved by the adaptive pilot gain are approximately the values listed in table 2 for each scenario, marked on the plots as dashed lines. Third, the gain converges rapidly, within the approximately 5 seconds that reference 5 specifies as typical for human pilot adaptation.
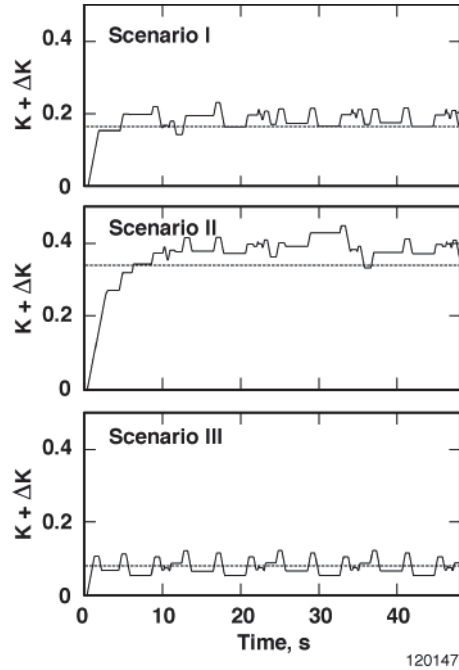

Figure 17. Pilot gain adaptation for changes in loop gain (dashed line is expected value).

Simulation results for scenarios IV and V in which the short period damping characteristics of the plant have been altered are shown in figure 18. The adaptive pilot gain in the case of increased damping (scenario V) shows the same well-behaved characteristics that were evident when adapting to changes in loop gain. The results for the decreased damping in scenario IV are quite different.
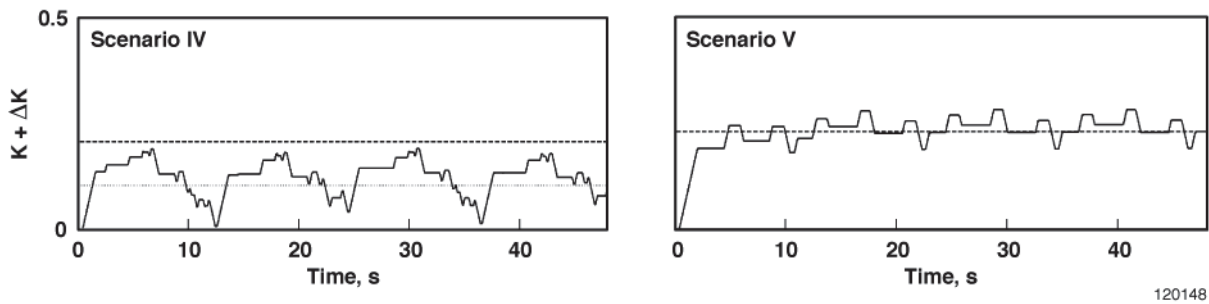

Figure 18. Pilot gain adaptation for changes in damping (dashed line is expected value).

16

Recall from figure 10 that eliminating the lag-lead filter for scenario IV results in either insufficient attenuation of the resonant peak for the corresponding pilot gain in table 2, or adequate attenuation, but significantly reduced bandwidth if the pilot gain is reduced by half. The results for scenario IV in figure 18 indicate that the adaptive pilot gain is alternating between the table 2 value (dashed line) and the reduced value (dotted line). The effects of these alternating gain values are also evident from the time history data in figure 19. Highly oscillatory pitch angle tracking occurs during those periods of the maneuver when the adaptive pilot gain is high. The regions of reduced pilot gain, which from figure 18 can be seen to occur near the 13, 25, and 36 second points in the data, result in a lagged, attenuated response. Incorporation of a self-tuning lag-lead filter, if appropriate adaptation rules can be found, may improve the convergence characteristics of the adaptive pilot gain and produce results more similar to the human subject data.
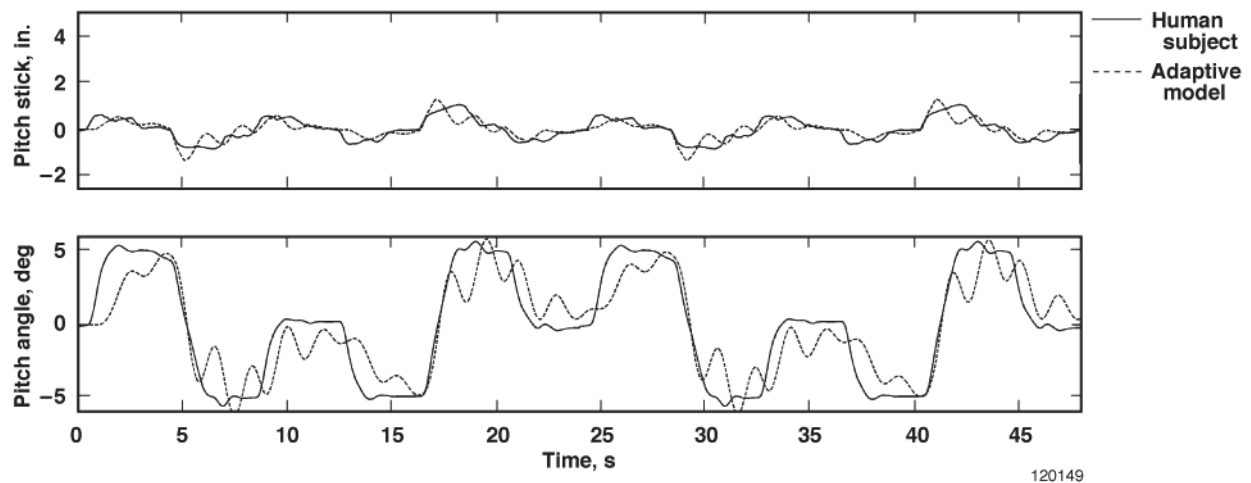

Figure 19. Comparison of adaptive pilot model to human subject for scenario IV.

Simulation results for scenarios VI and VII in which the short period natural frequency of the plant has been changed are shown in figure 20. In both cases the adaptation characteristics of the pilot gain are well-behaved. Note that, for scenario VII the pilot gain does not approach the value listed in table 2 and shown in the figure as a dashed line. Rather, it converges to a value of approximately 0.3 (dotted line), which was shown in figure 14 to produce the desired crossover slope and bandwidth without lead or lag compensation.
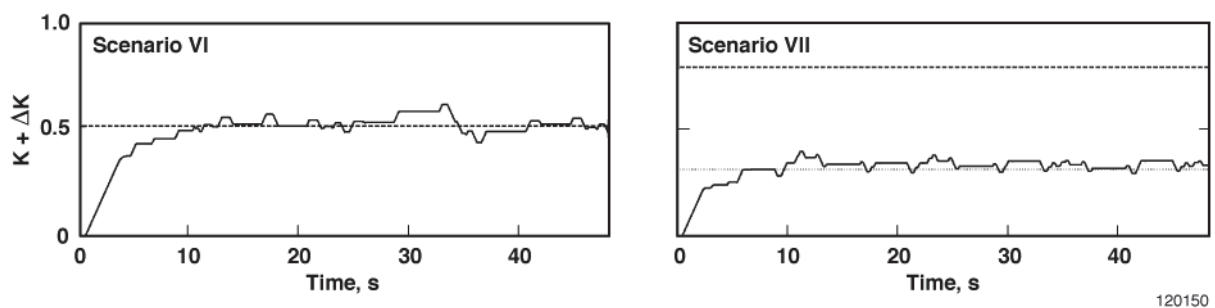

Figure 20. Pilot gain adaptation for changes in natural frequency.

17

Summary

The traditional crossover model of the pilot-vehicle system was shown to match human test subject piloting technique for pitch-axis, gross-acquisition tasks in a generic fighter aircraft. Furthermore, the pilot gain and lead-lag characteristics of the crossover model were successfully altered to match human subject piloting techniques for six scenarios of altered aircraft dynamics, including changes in loop gain, damping ratio, and natural frequency.

For the nominal aircraft dynamics and four of the six scenarios of modified dynamics, removal of the lead-lag portion of the pilot model did not significantly degrade its performance. In the case of an increase in natural frequency, removal of the lead-lag filter required a larger reduction in the pilot gain than when the filter was included in the model. In the case of a decrease in damping ratio, both the Neal-Smith handling qualities analysis and the human subject data showed that lag-lead compensation is an important component of the human subject's piloting technique. Removal of the lag-lead filter from the pilot model and a decrease in pilot gain produced a plausible crossover model for this scenario, albeit one that did not match the human subject's technique. In each case, then, it was deemed reasonable to model the pilot as a gain and a time delay.

A self-tuning pilot model was created by adding an adaptive term to the crossover pilot model gain. The update rule for the pilot gain was developed in an ad hoc manner and tuned to match the human subject's adaptation to changes in loop gain. In six of the seven dynamics scenarios, the self-tuning pilot model gain quickly converged to its expected value and remained fairly constant. In the case of a reduction in the aircraft's damping ratio, the adaptive pilot gain tended to alternate between a high and a low value. The resulting pilot-vehicle dynamics for this scenario consequently alternated between oscillatory and sluggish tracking response.

The adaptive pilot crossover model developed in this report provides a tool to aid in the analysis of pilot interactions with adaptive flight control systems. It is not a one-size-fits-all model and does not model every type of piloting technique, particularly in cases of lightly-damped aircraft dynamics. The inclusion of an adaptive term for pilot lag-lead compensation, which remains an open area of investigation, should improve the utility of this tool. Other work that remains to be done is to determine the extent to which this algorithm can model pilots of different types, and to determine the applicability of this algorithm to the pilot's control of the lateral axis.

References

1. McRuer, Duane T., and Henry R. Jex, "A Review of Quasi-Linear Pilot Models," *IEEE Transactions on Human Factors in Electronics*, Vol. 8, No. 3, September 1967, pp. 231-249.

2. Hess, R. A., "A Model for the Human's Use of Motion Cues in Vehicular Control," *Journal of Guidance, Control and Dynamics*, Vol. 13, No. 3, May-June 1990, pp. 476-482.

3. Bosworth, John T., and Peggy S. Williams-Hayes, "Stabilator Failure Adaptation from Flight Tests of NF-15B Intelligent Flight Control System," *Journal of Aerospace Computing, Information and Computing*, Vol. 6, March 2009, pp. 187-206.

4. Hanson, Curt, Jacob Shaefer, John J. Burken, Marcus Johnson, and Nahn Nguyen, "Handling Qualities Evaluations of Low Complexity Model Reference Adaptive Controllers for Reduced Pitch and Roll Damping Scenarios," AIAA-2011-6607, August 2011.

5. Hess, Ronald A., "Candidate Structure for Modeling Pilot Control Behavior with Sudden Changes in Vehicle Dynamics,"AIAA-2009-5608, August 2009.

6. McRuer, Duane, Irving Ashkenas, and Dunstan Graham, *Aircraft Dynamics and Automatic Control*, Princeton University Press, Princeton, New Jersey, 1973.

7. U.S. Department of Defense, *Military Standard Flying Qualities of Piloted Vehicles*, MIL-STD-1797, March 1987.

8. Hodgkinson, John, *Aircraft Handling Qualities*, AIAA Education Series, American Institute of Aeronautics and Astronautics, Reston, Virginia, 1999.